古 脊 椎 动 物 学 报
VERTEBRATA PALASIATICA

DOI: 10.19615/j.cnki.2096-9899.260411

CSTR: 32090.14.j.cnki.2096-9899.260411

Two anurognathid pterosaur specimens from the Yanliao Biota and a new interpretation of anurognathid skulls

TONG Shi-Da[1,2] JIANG Shun-Xing[1] CHENG Xin[3*] WANG Xiao-Lin[1,2*]

(1 *Key Laboratory of Vertebrate Evolution and Human Origins*, *Institute of Vertebrate Paleontology and Paleoanthropology*, *Chinese Academy of Sciences* Beijing 100044)
(2 *College of Earth and Planetary Sciences*, *University of Chinese Academy of Sciences* Beijing 100049)
(3 *College of Earth Sciences*, *Jilin University* Changchun 130061)
* Corresponding authors: chengxin@jlu.edu.cn, wangxiaolin@ivpp.ac.cn

Abstract Anurognathids are a clade of small, early-diverging non-pterodactyloid pterosaurs distributed across Eurasia from the Middle Jurassic to the Early Cretaceous. Their defining characteristic is a short and broad skull, a morphology distinct from all other pterosaur clades. Due to limited preservation, the cranial anatomy of this group has long been difficult to understand in detail. In this study, we provide a detailed description of two anurognathid specimens from the Tiaojishan Formation of the Yanliao Biota. The relatively well-preserved skull of one specimen was reconstructed through computed tomographic scanning. This reveals a unique skull element, possibly functionally analogous to the supraorbital bone of varanid lizards. The CT reconstruction offers new insights into the anurognathid skull. Based on these findings, we revised the skulls of previously described taxa, ultimately integrating them into a new reconstruction for this clade. We present a detailed comparative analysis and discussion of the postcranial osteology within Anurognathidae.

Key words Yanliao Biota, Tiaojishan Formation, Pterosaur, Anurognathid, *Cascocauda*

Citation Tong S D, Jiang S X, Cheng X et al., in press. Two anurognathid pterosaur specimens from the Yanliao Biota and a new interpretation of anurognathid skulls. Vertebrata PalAsiatica. DOI: 10.19615/j.cnki.2096-9899.260411

1 Introduction

Anurognathids were a strange group of small pterosaurs that lived during the Middle Jurassic to Early Cretaceous of Eurasia. They had many unique features compared to other pterosaurs: a short and broad skull, huge orbits, and a wing finger capable of flexion at all joints (Hone, 2020; Wei et al., 2021; Yang et al., 2021). Due to their unique head structure, they are generally considered to be insectivores in low-light environments (Bennett, 2007; Ősi, 2010). Some species exhibit distinct arboreal characteristics (Lü et al., 2017).

国家自然科学基金(批准号：42072017, 42288201, 42572026)。
收稿日期：2026-03-02

Up to now, this group includes eight species, and 14 specimens have been reported. The first anurognathid discovered was *Anurognathus ammoni*, reported from the Solnhofen limestone of Bavaria and is represented by two specimens (Döderlein, 1923; Bennett, 2007). The second species found was *Batrachognathus volans* from the Karabastau Formation of Kazakhstan (Riabinin, 1948). Since then, another six species of anurognathids, *Dendrorhynchoides curvidentatus*, *Jeholopterus ningchengensis*, *Luopterus mutoutdengensis*, *Vesperopterylus lamadongensis*, *Sinomacrops bondei* and *Cascocauda rong*, have been reported from the Jehol and Yanliao biotas, northeastern China. The two species from the Jehol Biota are *Dendrorhynchoides* from the Yixian Formation and *Vesperopterylus* from the Jiufotang Formation. Of the other four species from the Yanliao Biota, *Jeholopterus* is from the Daohugou Bedding (Haifanggou or Jiulongshan Formation), and the remaining three species are from the Linglongta Bedding (Tiaojishan Formation). In 2023, a specimen from the Sinuiju Biota of North Korea was also identified as *Jeholopterus* (So et al., 2023), although it was reported in 2009 (Gao et al., 2009). Also, there are two indeterminate specimens, including IVPP V16728 from the Linglongta Bedding of the Yanliao Biota (Tiaojishan Formation) and fragmentary wing bones of one individual from the Bakhar Formation (Unwin and Bakhurina, 2000). Bennett also mentioned that the sacrum of the holotype of *Mesadactylus* is similar to that in *Anurognathus* (Bennett, 2007).

The phylogeny of Anurognathidae is controversial, with a long ghost lineage of anurognathids, and it is difficult to determine their specific phylogenetic position within pterosaurs. At present, there are mainly the following hypotheses: they are at the basal branch of the Pterosauria (Kellner, 2003; Lü and Ji, 2006; Bennett, 2007; Wang et al., 2009, 2014, 2017); between the Dimorphodontidae and the Campylognathoididae (Unwin, 2003); a sister-group of the Pterodactyloidea (Andres et al., 2010); a sister-group of the Monofenestrata (Vidovic and Martill, 2018); the basal branch of Monofenestrata, the sister-group of the clade with Darwinoptera and Pterodactyloidea (Wei, 2021); or they are a sister-group of Breviquartossa, outside of Monofenestrata (Yang et al., 2021). This confusion is due to poor preservation, as their slender bones make it difficult to determine the condition of their skull fenestration patterns. At first, the skull was reconstructed with separate narial, antorbital, and orbital fenestrae, and some researchers still support this reconstruction (Wellnhofer, 1975; Bennett, 2007; Hone, 2020; Yang et al., 2021). Others considered that anurognathids might have a confluent external naris and antorbital fenestra, which is referred to as a nasoantorbital fenestra (Andres, 2010; Vidović and Martill, 2018; Dalla Vecchia, 2009, 2019; Wei, 2021). Dalla Vecchia (2022) considered that the skull fenestration pattern is unique; the bar separating the orbit and the antorbital fenestra is absent, forming a large orbitoantorbital fenestra. This still needs to be determined in a specimen preserving the complete skull, so this work did not factor in the phylogenetic analysis. Here we report two new specimens of Anurognathidae: IVPP V26040 from the Tiaojishan Formation

of Linglongta, Jianchang, Huludao, Liaoning, northeastern China and IVPP V23669 from the Tiaojishan Formation of Qinglong, Hebei, northern China. These two new specimens provide new information for the group, including a new record of an anurognathid sternum exposed in ventral view, and a unique structure of their skull.

2 Materials and methods

Pterosaur specimens IVPP V26040 and V23669 described here are housed at the Institute of Vertebrate Paleontology and Paleoanthropology, Chinese Academy of Sciences (IVPP).

X-ray micro-computed tomography (CT) To optimize the scanning resolution, the skull of the specimen IVPP V23669 was isolated from the slab. The skull was scanned using the industrial CT scanner Phoenix v-tome-x at the Key Laboratory of Vertebrate Evolution and Human Origins, IVPP, with a beam energy of 140 kV and a flux of 70 μA at a resolution of 9.063 μm per pixel. The raw CT data were completed with Mimics (Materialise Medical Co, Belgium version 19.0) for 3D reconstruction and measurements.

Institutional abbreviations BSP, Bayerische Staatssammlung für Paläontologie und Geologie, Munich, Germany; CAGS, Chinese Academy of Geological Sciences, Beijing, China; CKGP, Kim Il Sung University, Pyongyang, Democratic People's Republic of Korea; GMV, National Geological Museum of China, Beijing, China; IVPP, Institute of Vertebrate Paleontology and Paleoanthropology, Chinese Academy of Sciences, Beijing, China; JZMP (JPM), Jinzhou Paleontological Museum, Jinzhou, China; NHMC (BMNHC), Natural History Museum of China, Beijing, China; NHMUK, The Natural History Museum, London, UK; NJU, Nanjing University, Nanjing, China; PIN, Palaeontological Institute, Russian Academy of Sciences, Moscow, Russia; SMNS, Staatliches Museum for Naturkunde Stuttgart, Stuttgart, Germany.

3 Systematic paleontology

Anurognathidae Kuhn, 1937

***Cascocauda* Yang et al., 2021**

***Cascocauda rong* Yang et al., 2021**

Holotype NJU-57003, preserving a well-articulated and nearly complete skeleton with extensive preserved soft tissues. The specimen comprises two fragmented slabs (the main slab and the counter slab), which are housed at Nanjing University, Nanjing, China.

Referred specimens IVPP V23669, a nearly complete, articulated skeleton exposed in ventral view; V26040, also a nearly complete articulated skeleton without the anterior part of the skull and right forelimb, which is exposed in ventral view.

Diagnosis At least 17 caudal vertebrae with elongate zygapophyses and chevrons, scapula slightly longer than the coracoid, the second phalanx of wing finger is more than twice

the length of the third one, the second phalanx of pedal digit V curved, the upper and lower jaws each have seven sets of teeth, the anterior teeth of the premaxilla, maxilla and mandible are long and thin with distally curved, whereas the posterior mandibular teeth are short and hook-shaped (modified from Yang et al., 2021).

Type locality and horizon Mutoudeng, Qinglong County in Hebei Province, China, from the Middle-Upper Jurassic Tiaojishan Formation (NJU-57003, IVPP V23669).

Additional locality Linglongta, Jianchang, Huludao, Liaoning, China; Middle-Upper Jurassic Tiaojishan Formation (IVPP V26040).

Notes Given the close correspondence in postcranial size and proportions between IVPP V23669, V26040, and the holotype, these specimens are assigned to the same taxon. The lack of integumentary filamentous structures is likely due to their poor preservation. The discrepancy in caudal vertebral count may be attributed to individual variation.

4 Description

4.1 IVPP V23669

The right forelimb is positioned over the posterior portion of the skull. Only parts of the wing finger phalanges are preserved. The right hind limb is detached and appears rotateds. (Figs. 1–5).

Ontogenetic status The scapula and coracoid are unfused. This indicates the specimen is a juvenile.

Skull To preserve the fossil, the skull was detached along the natural fracture in the rock matrix for CT scanning. Ventral anatomy was studied directly from the specimen (with CT supplement), whereas dorsal anatomy was primarily from CT data. Due to severe compaction, many skeletal elements are thoroughly fused, making their individual boundaries nearly indistinguishable. Therefore, only their approximate outlines could be identified in the reconstruction.

The skull has been compressed towards the left. As a result, the premaxilla was displaced posteriorly. The left maxilla underwent a counterclockwise rotation along its mid-shaft axis, resulting in its inversion. This rotation caused the palatine bone, which articulates with the ventral surface of the maxilla, to become exposed dorsally. In contrast, the right maxilla remained articulated with the premaxilla. The cranial block, including the occipital region, was displaced anterolaterally (forward and to the left), likely due to direct pressure from the right forelimb. Concurrently, torsional forces affected the palatal region, causing some rod-like bones to protrude from the right side. These elements now overlie the ascending processes of both the premaxilla and the right maxilla. Regarding the mandibles, the left dentary is comparatively well-preserved, whereas the posterior portion of the right mandible is fractured and translationally displaced.

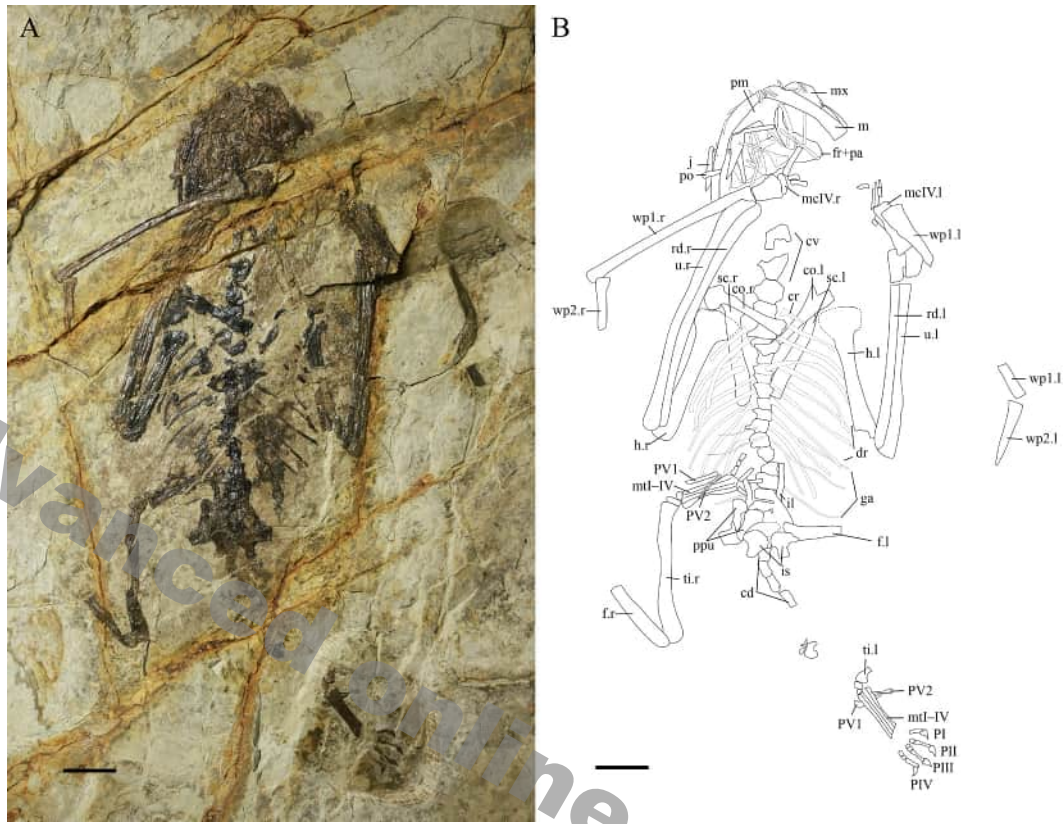

Fig. 1 Overview photograph (A) and line drawing (B) of the specimen IVPP V23669 from the Middle-Upper Jurassic Qinglong, Hebei
Abbreviations: cd. caudal vertebra; co. coracoid; cr. cervical rib; cv. cervical vertebra; dr. dorsal rib; f. femur; fr. frontal; ga. gastralia; h. humerus; il. ilium; is. ischium; j. jugal; l. left; m. mandible; mcIV. metacarpal IV; mtI–V. metatarsal I–V; mx. maxilla; pa. parietal; pm. premaxilla; po. postorbital; ppu. prepubis; PI–IV. pedal digits I–IV; PV1 and 2. phalanges 1 and 2 of pedal digit V; r. right; rd. radius; sc. scapula; ti. tibia; u. ulna; wp1–2. wing phalanges 1–2. Scale bars equal 10 mm

Premaxilla The premaxilla in specimen IVPP V23669 has been significantly displaced posteriorly. Most teeth, except for a few isolated ones, have been shed. The shed teeth are primarily situated along the ventral margin of the mandible and are inflected medially, making it very difficult to identify the precise boundaries of the premaxilla. Even in CT scans, the bone sutures remain indistinct due to compaction. Consequently, only the regions that can be definitively identified are illustrated here (Figs. 2, 3A). The overall morphology of the premaxilla conforms to the characteristic T-shaped configuration observed in other anurognathids. It extends posteriorly into a relatively robust and elongate bony strut, which constitutes the median process of the rosturm. This process measures approximately one-half of the total skull length. In BSP 1922 I 42 (the holotype of *Anurognathus ammoni*), this ascending process is visible in lateral view. In both of the specimens GMV 2128 and SMNS 81928, the process is fractured and exhibits rotation.

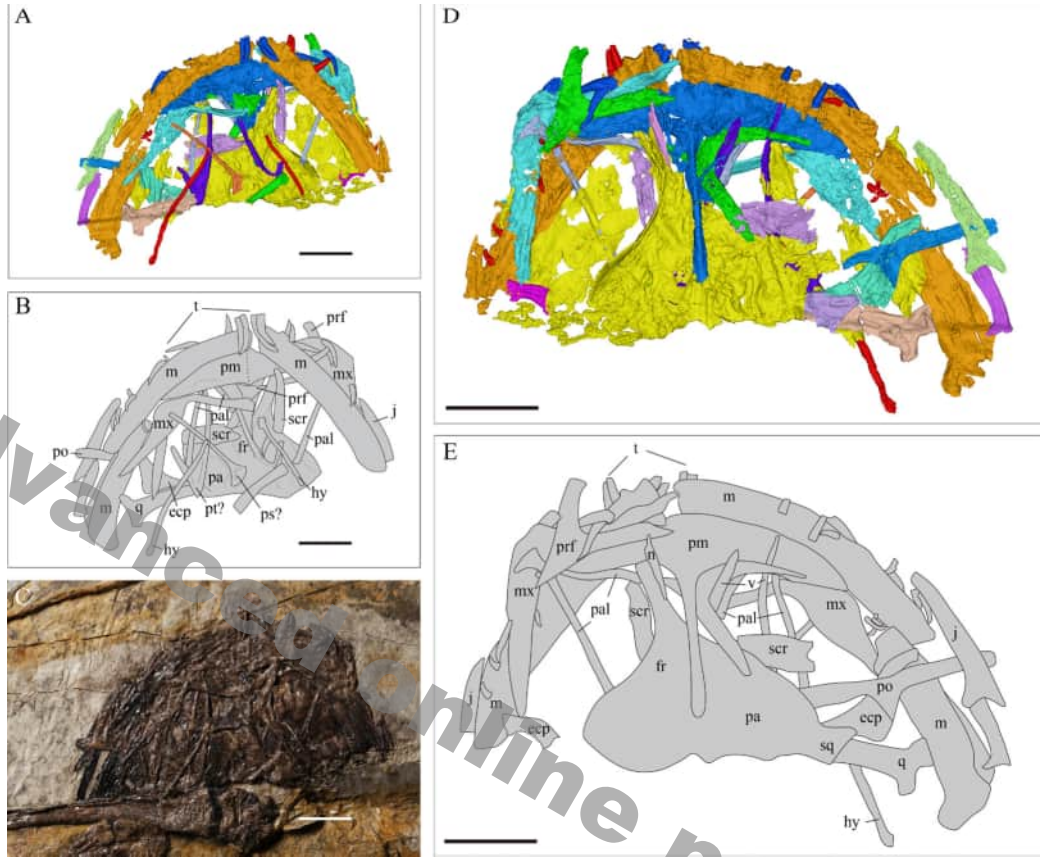

Fig. 2 The cranium of specimen IVPP V23669 from the Middle-Upper Jurassic Qinglong, Hebei
A–C. the digital reconstruction (A), line drawing (B), and photograph (C) of the skull in ventral view;
D, E. the digital reconstruction (D) and line drawing (E) in dorsal view
Abbreviations: ecp. ectopterygoid; fr. frontal; hy. hyoid; j. jugal; m. mandible; mx. maxilla; n. nasal; pa. parietal; pal. palatine; pm. premaxilla; po. postorbital; prf. prefrontal; ps. parasphenoid; pt. pterygoid; q. quadrate; scr. sclerotic ring; sq. squamosal; t. tooth; v. vomer. Scale bars equal 5 mm

Maxilla The maxilla is highly susceptible to distortion and is preserved as an elongated, arcuate bone bearing at least four teeth. An ascending process is present anteriorly, articulating with the premaxilla to form the external naris. As with the premaxilla, severe compression obscures its original morphology. However, the orientation of the retained teeth on both the left and right maxillae suggests they remain aligned with the overall dorsoventral plane of the skull (Figs. 2, 3B). The following description is based primarily on the disarticulated maxilla of GMV 2128 for reference (Ji and Ji, 1998, 1999). In PIN 52-2, the maxilla appears triradiate. The short anterior ramus is the premaxillary process of the maxilla, and the vertical ramus corresponds to the ascending process of the maxilla. The ascending process extends almost perpendicularly to the premaxillary contact surface. The posterior ramus is strap-like, tapering distally, with a slight dorsal and medial arch. Its distal termination is obscured by overlying elements (Dalla Vecchia, 2022). In IVPP V12705, the ascending process is also

nearly perpendicular to the main body of the maxilla (Wang et al., 2002). In GMV 2128, the ascending process of the maxilla is not perpendicular to the posterior ramus. Although both sides in IVPP V23669 exhibit displacement, this angular deviation of the ascending process is pronounced in the left maxilla. In the right maxilla, which has been displaced posteriorly, the angular alteration is less severe. Based on the better-preserved specimens, PIN 52-2 and IVPP V12705, it is inferred that the ascending process of the maxilla likely projected at a near-perpendicular angle in life. The anterior ramus is not observable in GMV 2128 and IVPP V23669. The posterior ramus, while also tapering, terminates in a distinct, pointed tip. Considering that the posterior ramus of PIN 52-2 is overlain by the mandible, it is suggested that the maxilla in these specimens may also have terminated pointedly. The region where the maxilla tapers may present the articulation site with the jugal.

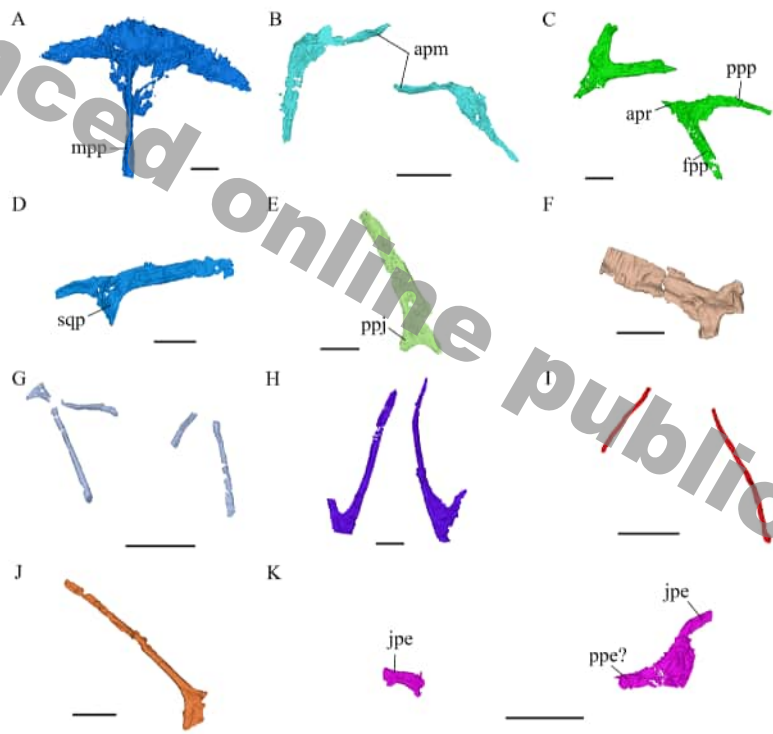

Fig. 3 Digital reconstruction of cranial elements of specimen IVPP V23669 in dorsal view (only J in ventral view) from the Middle-Upper Jurassic Qinglong, Hebei

A. premaxillae; B. left and right maxillae; C. left and right prefrontals; D. right postorbital; E. right jugal; F. right quadrate; G. left and right palatines; H. left and right vomers/pterygoids; I. left and right hyoids; J. parasphenoid; K. left and right ectopterygoids

Abbreviations: apm. ascending process of the maxilla; apr. apex of prefrontal; fpp. frontal process of prefrontal; jpe. jugal process of ectopterygoid; mpp. median process of premaxilla; ppe. pterygoid process of ectopterygoid; ppj. postorbital process of jugal; ppp. posterior process of prefrontal; sqp. squamosal process of postorbital. Scale bars equal 2 mm (A, C, D, E, F, H and J) and 5 mm (B, G, I and K)

Mandible The posterior portion of the left mandibular ramus is missing. The right mandibular ramus is fractured at mid-length, likely due to compression from the right forelimb, resulting in medial displacement of its posterior segment. Based on the in situ-preserved anterior sections, the mandible exhibits a comparatively gentle curvature

Teeth The CT reconstruction and the impression of the specimen reveal approximately thirty teeth in V23669. Eleven of these are located in the premaxilla. Ten premaxillary teeth are discernible in the CT data (Fig. 4); only one tooth on the right side remains in articulation with the premaxilla, and all others are shed. An additional premaxillary tooth is preserved only as an impression on the right side.

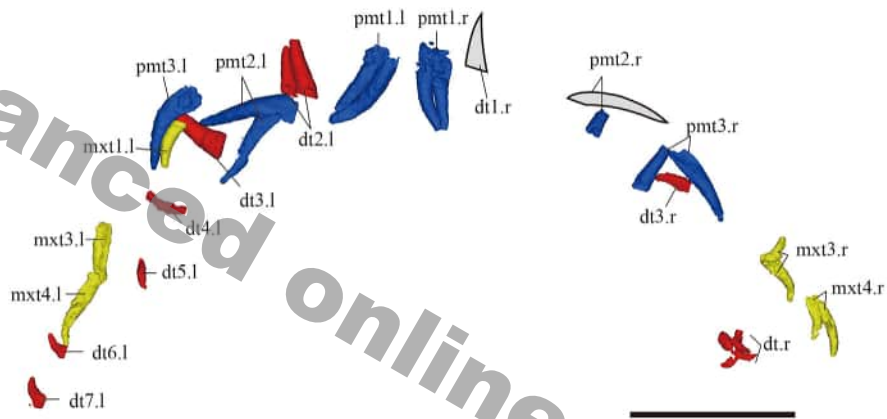

Fig. 4 The digital reconstruction of the teeth in specimen IVPP V23669 in dorsal view from the Middle-Upper Jurassic Qinglong, Hebei
Abbreviations: dt. dentary tooth; l. left; mxt. maxillary tooth; pmt. premaxillary tooth; r. right
Scale bar equals 5 mm

The premaxillary dentition can be interpreted as comprising three sets on each side. The anteriormost four teeth (constituting two sets) are recurved and lie ventral to the mandible, with their roots preserved as impressions. The consistent apical orientation of these impressions indicates that they represent closely appressed premaxillary teeth, not an admixture with mandibular elements, and are therefore considered discrete sets. On the left side, one nearly complete premaxillary tooth has its crown obscured by the left maxilla. An adjacent tooth, displaced dorsally and overlying the maxilla, likely forms a set with the former. A third tooth of comparable length is displaced laterally by the left maxilla; as its root is not fused to the maxilla, it is identified as the third set of teeth on the left premaxilla. Four premaxillary teeth are preserved on the right side: one retains its original orientation (only root left) in proximity to a transversely oriented premaxillary tooth impression, while two additional, complete teeth are present as a closely associated pair, with one in its original position and the other transversely oriented.

The left maxilla preserves three isolated, subequal teeth, all of which are smaller than the premaxillary teeth (the latter appear incomplete in CT reconstruction, particularly the

anteriormost four, which exhibit distinct root impressions in the specimen). On the right side, displacement has resulted in four maxillary teeth preserved as two sets situated lateral to the right mandible. Based on their sizes and positions relative to the mandible, these displaced right maxillary teeth are likely the same as the posterior two maxillary teeth preserved on the left side.

The left mandible preserves seven teeth. The anterior two are closely appressed, while the remaining five are isolated. Reference to impressions in the specimen indicates a posteriorly decreasing size within the row of mandibular teeth. The ultimate and penultimate left mandibular teeth are distinctly short, and hook-shaped. The right mandible preserves four teeth and one impression. The tooth situated near the right third premaxillary set can be identified as the third right dentary tooth. An impression at the anteriormost extent of the right mandible, positioned anterior to the first left mandibular set, is designated the first right dentary tooth. The remaining three teeth are clustered within a gap caused by mandibular fracturing: two are of similar length—significantly smaller than the ultimate maxillary teeth but comparable to the left fourth dentary tooth—while the third is distinctly short, hook-like (indicated in red in Fig. 4), resembling the left sixth and seventh mandibular teeth. The mandibular dentition of IVPP V23669 exhibits notable heterodonty: the anterior four to five teeth are elongate, slender, with apically curved crowns and straight roots, whereas the posterior teeth diminish in size, with the last two assuming a short, hook-like morphology. However, the crowns of these posterior, hook-shaped teeth do not differ substantially from those of the anterior, slender teeth. Therefore, a functional differentiation within the teeth based on shape is not supported by the available evidence.

Based on the specimen, the premaxilla likely possessed three paired tooth positions per side. By integrating data from both mandibular rami and considering the closely appressed anteriormost left pair as a single position, the mandible is inferred to have borne approximately seven tooth positions per side. Although maxillary tooth positions are obscured by displacement, the preserved elements align with putative occlusal positions corresponding to mandibular teeth 4, 6, and 7, suggesting the presence of at least four maxillary tooth positions.

The specimen exhibits numerous sets of similarly sized teeth. This includes all left premaxillary sets (two sets), all right premaxillary sets (three sets), the second left mandibular set, the first left maxillary set, and the two preserved right maxillary sets. These sets may represent replacement teeth; this condition is also present in *Cascocauda*. However, in IVPP V23669, many sets of teeth are very similar in size, except for the third and fourth right maxillary teeth, which show a marked disparity. Erupting replacement teeth were not observed in the CT data.

Frontal and parietal These elements are discernible only through CT reconstruction, presenting a roughly fan-shaped structure. The anteriormost portion forms a subtriangular area, which, based on comparison with specimen SMNS 81928, is tentatively identified as

the frontal. The posterior region is accordingly interpreted as the parietal. However, due to distortion and the thin nature of the bones themselves, the precise position of the suture between these elements cannot be delineated (Fig. 2).

The posterior extent of this complex is not preserved. A projection extending laterally on the right side may represent a portion of the squamosal. The anterior region of the putative frontal is highly fragmentary, allowing only recognition of its general contour. An adjacent, subtriangular bony fragment in proximity may pertain to the nasal.

Prefrontal IVPP V23669 preserves a unique paired structure. The left element lies close to the ascending process of the left maxilla, near the anterior orbital margin. However, due to lateral displacement of the left premaxilla, its original position and orientation (dorsal/ventral) are ambiguous. The right element is partially overlain by the displaced ascending process of the premaxilla, similarly, obscuring its original placement. Yet, as surrounding elements have undergone primarily translational displacement, it is inferred that the overall dorsoventral orientation of the skull is maintained (Figs. 2, 3C).

Review of other specimens reveals that the same structure is present in nearly all anurognathids. In CAGS-Z070 (Ji and Yuan, 2002), bilateral impressions are preserved on the skull roof, with a V-shaped apex pointing anteriorly. One ramus may contact the frontal; the left appears unattached, while the right apex may contact the maxillary ascending process and another ramus the premaxillary ascending process. In IVPP V12705A, a bone fragment previously identified as the right maxillary ascending process may instead belong to this element, as it is not fused to the maxilla. In IVPP V12705B, a bone fragment on the skull roof connects with the fragment in part A, together forming a V-shaped structure with an angle of approximately 70°. Dalla Vecchia (2022) noted PIN 2585/4a has an element posterior to the maxillary ascending process, suggesting it could be a nasal (anterior or anterodorasal to the maxilla), a lacrimal, or supraorbital. The figure illustrates bilateral traces: a V-shaped apex anteriorly and a ramus contacting the frontal. In SMNS 81928, a triangular bone identified by Bennett as a prefrontal may represent the apical remnant of this element (Bennett, 2007). In IVPP V23669, the size of this element precludes its identification as a nasal. If it were lacrimal, one would expect an articulation with the jugal, but no additional ascending process is observed in the maxillary region. Its pointed end could theoretically represent a broken extension of the lacrimal-jugal articulation, with the blunt end articulating with the frontal. However, such an extension would be expected to lie ventral to the sclerotic ring and should be visible in specimens like SMNS 81928 where the ring is well-preserved. Otherwise, its absence would likely have caused disruption or displacement of the overlying sclerotic ring. However, no such disruption is evident, and the element itself is not discernible in specimen SMNS 81928. The preservation of only the apical portion in this specimen suggests this branch lies dorsal to the sclerotic ring. Therefore, this structure is interpreted here as a distinct element, possibly formed by the fusion of the prefrontal and supraorbital bones, situated dorsally above

the orbit. Its previous absence in descriptions may be due to its weak connection to surrounding bones, making it prone to detachment and displacement during taphonomic processes.

Furthermore, based on this revised interpretation, the bone previously identified as the frontal or lacrimal in BSP 1922 I 42 may instead be this "prefrontal" element (Bennett, 2007; Döderlein, 1923; Wellnhofer, 1975). The left element in that specimen is exposed in lateral view, showing a deformed and ventrally deflected apex, a posteriorly tapering ramus, and a broken base where another ramus is missing. The right element is preserved in dorsal view, retaining only a posteriorly tapering ramus; its possible curvature is uncertain, and an anterior pit may indicate the loss of the apex and the other ramus.

This element is described as follows: it presents a bifurcated, V-shaped structure forming an angle of approximately 60°. The apex of the structure may articulate with the ascending process of the maxilla. One ramus may have contacted the anterior margin of the frontal. The other, longer ramus extends posteriorly, tapering to a point and likely terminates naturally near the posterior margin of the frontal.

A potentially homologous structure is reported in other pterosaurs. A similar element in the orbital region was identified as a supraorbital in *Dimorphodon macronyx* (specimen NHMUK 41212) (Sangster, 2021). This bone originates from the ventrolateral part of the frontal, featuring a long, curved process that extends posteromedially into the orbital cavity, likely terminating near its center—a morphology consistent with observations in anurognathids. However, Sangster interpreted this process as extending medially, contrasting with the posterior orientation observed in anurognathids like BSP 1922 I 42. It is plausible that the orientation of this element in the *Dimorphodon* specimen (NHMUK 41212) may be caused by compression caused by metacarpal IV and that its in *vivo* orientation was likely posterolateral.

As Sangster noted for *Dimorphodon macronyx*, the morphology of this element in anurognathids closely resembles the supraorbital (or palpebral) bones found in extant lepidosaurs (e.g., *Varanus komodoensis*). It likely served a similar function: protecting the anterior and dorsal aspects of the enormous eye and helping to secure it within the orbit (Kubota et al., 2024).

Jugal An elongate bone fragment, which widens posteriorly, is preserved overlying the postorbital. Its posterior end exhibits both a posterior process and an ascending process. The ascending process is interpreted as articulating with the postorbital, supporting its identification as the jugal. Its anterior end shows no trace of a lacrimal process and appears to extend into the tooth-bearing region. This suggests that the jugal may have extended anteriorly, overlapping with the maxilla for a considerable distance (Figs. 2, 3E). As most teeth are found lateral to this structure, the jugal is inferred to have lain medial to the maxilla. This medial overlap is likely initiated at the point where the maxilla begins to taper. The absence of a lacrimal process on the jugal further supports Dalla Vecchia's hypothesis that the orbit and antorbital fenestrae

form a large, confluent orbitoantorbital fenestra.

Postorbital The specimen preserves a triradiate bone that corresponds morphologically to the postorbital described in SMNS 81928 (Figs. 2, 3D). However, due to severe compression of the element, morphological details cannot be discerned. The posterior ramus appears to originate from approximately the dorsal one-third of the height of the bone. It extends posteriorly to articulate with the squamosal; CT reconstruction suggests its distal end curves slightly dorsally, forming a flange-like process. Its dorsal and ventral margins contacted the frontal and jugal.

Quadrate This element is severely compressed by the overlying right forelimb. Nonetheless, its position and general outline permit identification as the quadrate. The posterior aspect exhibits two distinct projections, although their full extent is obscured by compression (Figs. 2, 3F).

Based on comparison with the better-preserved dorsal and ventral components of the quadrate in GMV 2128, it can be determined that the quadrate was elongated, having a columnar morphology. Its ventral (mandibular) extremity formed three condyles for articulation with adjacent elements: a larger, more expanded condyle for the quadratojugal, a mandibular condyle, and a smaller medial condyle for the pterygoid.

Squamosal Bennett (2007) identified a sigmoidal bone extending laterally from the parietal in SMNS 81928 as the squamosal, suggesting its terminus articulated with the squamosal process of the postorbital and the presence of a relatively large squamosal flange extending posteriorly or posteroventrally from the middle of the bone. In BSP 1922 I 42, where the skull is exposed in lateral view, Bennett (2007) identified a bone situated posterior to the maxilla and ventral to the main skull roof as the left squamosal.

However, more complete morphology is observable in GMV 2128 and CAGS-Z070. Putative fragments are also present in IVPP V12705 (possibly the posterior portion) and JZMP-07-04-3 (possibly the anterior, S-shaped region). Crucially, this element consistently articulates with the jugal in all known specimens. In GMV 2128 and SMNS 81928, it is overlain by the quadrate and postorbital. In IVPP V12705, it lies on the hyoid apparatus but is clearly overlain by the palatine.

These preserved positions are inconsistent with its identification as the squamosal. The identification in SMNS 81928 may be due to the parietal overlying the medial portion of this bone. In IVPP V23669, the expanded posterior end of the right element is visible ventrally. The left sigmoidal element is revealed through the CT data. The right posterior portion is overlain by the postorbital and a curved bone extending from the parietal, while its anterior part is exposed dorsal to the mandible (Fig. 2).

This suggests that the curved bone extending from the parietal may be the true squamosal. The sigmoidal bone previously identified as the squamosal, which also contacts the jugal and is overlain by other elements, is reinterpreted here as potentially belonging to the

palatal region, possibly representing the ectopterygoid. Due to preservational limitations, the exact nature of these contacts remains ambiguous. A conservative approach is adopted here, assuming potential minor displacement of the element and proceeding with the analysis under the premise that the squamosal articulated with the squamosal process of the postorbital.

Hyoid The right hyoid is only partially preserved, likely representing less than half of its original length. Approximately two-thirds of the left hyoid is observable directly on the slab, with its posterior portion obscured by the right forelimb. CT scans reveal its near-complete length, which is approximately two-thirds that of the mandible (Figs. 2, 3I).

Palatine The left palatine is visible in ventral view in the specimen and dorsal view in CT scans. Its anterior region and two anterior rami are well-preserved, while the posterior ramus is fractured as observed ventrally. The right palatine is fractured due to displacement of the right maxilla. Its transverse ramus lies adjacent to the ascending process of the right maxilla. The posterior ramus overlies both the maxillary ascending process and the putative parasphenoid. Both left and right posterior rami are rod-like anteriorly, flaring slightly posteriorly into a strap-like morphology (Figs. 2, 3G).

Vomer/Pterygoid A long, slightly curved, rod-like bone is visible in ventral view in IVPP V23669. CT reconstruction of its dorsal aspect reveals that it extends nearly the full length of the skull and occupies the most ventral region (excluding the hyoid). This element is likely interpreted here as the fused or closely appressed vomer (anteriorly) and pterygoid (posteriorly) of the palate (Figs. 2, 3H).

The posterior region of this complex bears an anteriorly directed process. The area enclosed by the main rod and this process is filled with a distinct, thin, plate-like bony sheet. However, the termination of the anterior process and any potential articulation are not discernible. A slender, elongated bone from the posterior palatal region in IVPP V12705 may represent the same anterior process, supporting its identification here.

A second, similar rod-like bone is present in the mid-ventral region, also seemingly associated with a thin bony sheet and an anterior process. However, due to overlying elements and severe compaction, it cannot be confidently separated from surrounding structures even in the CT scans. It is tentatively interpreted as the contralateral vomer/pterygoid complex.

Parasphenoid A rod-like bone with a distinct bifurcation at its posterior end and a plate-like expansion is visible in ventral view. A similar, elongated rod-like element is present in the mid-posterior skull region of *Luopterus*. This morphological correspondence suggests a possible identification as the parasphenoid. However, the exceptionally long anterior process casts doubt on this interpretation (Figs. 2, 3J).

Ectopterygoid As proposed previously for the squamosal, the boomerang-shaped element in IVPP V23669, BSP 1922 I 42, GMV 2128, CAGS-Z070, IVPP V12705, and JZMP-07-04-3 is re-identified here as the ectopterygoid. Most specimens preserve it in dorsal view, while the element in BSP 1922 I 42 likely represents the right ectopterygoid in ventral view.

In IVPP V23669, only the sigmoidal portion of the left ectopterygoid is preserved. On the right side, the posteromedial expansion of the mid-section of the bone is visible ventrally. CT reconstructions of the dorsal surface reveal the sigmoidal portion, but the rest is obscured by the overlying postorbital and squamosal (Figs. 2, 3K). However, based on GMV 2128, the complete morphology of the element is boomerang-shaped. Its anterior end, articulating with the jugal, forms a sigmoidal curve. The mid-section expands noticeably, while the posterior portion tapers again and extends medially, likely to articulate with the pterygoid.

Vertebral column The anterior cervical vertebrae are not preserved. Approximately five posterior cervical vertebrae are present in poor condition. Some centra exhibit visible transverse processes. A partially preserved, short eighth cervical rib is observable. The ninth cervical rib tapers distally and is comparable in length to the subsequent dorsal ribs. Individual centra are about 3.26 mm in length and 4.67 mm in width. The total length of the cervical series cannot be determined due to the disarticulation of the skull.

The anterior dorsal vertebrae are obscured by possible sternal remains. Based on dorsal rib counts, approximately 12 dorsal vertebrae and 9 pairs of dorsal ribs are present, with a total series length of 34.97 mm. The first three pairs of dorsal ribs curve posteriorly. Ribs 4–7 on the left side are straight or curve anteriorly, while those on the right remain posteriorly curved. Ribs 8 exhibit strong posterior curvature. The ninth dorsal rib is preserved only on the right side. Four pairs of gastralia are present: the anterior two pairs lie near dorsal vertebrae 8–9, while the posterior two are fractured and displaced, likely due to influence from the right hindlimb.

The sacral region comprises approximately five vertebrae. Two sacral ribs can be discerned: one is posteriorly inclined, while the other is transversely oriented. The posterior sacral vertebrae are obscured by the overlying prepubis, preventing detailed observation.

Nearly eight caudal vertebrae are preserved. They exhibit a posterior trend of gradual elongation and tapering. An impression of a chevron is observed in the matrix beyond the last preserved centrum. The distalmost preserved vertebra measures 2.35 mm in length. In other reported anurognathids with elongated tails, the caudal series typically comprises 15 to 20 vertebrae, with centrum length reaching its maximum in the mid-region of the series, suggesting a long and slender tail in this individual.

Pectoral girdle Most parts of the scapula and coracoid are preserved as impressions, with only the right coracoid complete. The scapula and coracoid are unfused. The distal end of the coracoid is expanded, forming a process approximately twice the width of its shaft. A distinct tubercle is present on the glenoid portion of the coracoid.

Forelimb The humerus is straight. The deltopectoral crest is preserved mostly as an impression and is trapezoidal in shape. The ulnar crest is not completely preserved, but its orientation relative to the shaft suggests it may have been triangular. The ulna and radius are straight and slender with subequal shaft diameters, and they diverge distally. Accurate

measurement is hampered by the missing proximal ends on the left and fractures on the right. The lengths of the right ulna and radius are approximately 1.63 times the length of the humerus. On the right side, the metacarpals are obscured by the wing phalanges. The distal portion of the fourth metacarpal is exposed. The proximal parts of manual digits I and II are preserved. The first phalanx of digit III overlies the skull, and the distal phalanges are not preserved. The pteroid is concealed beneath the entire right forelimb but is partially visible in the CT reconstruction as a slender element. On the left side, a robust fourth metacarpal, though also overlain by wing phalanges, is partially exposed laterally and overlies the other metacarpals. Only parts of the left manual phalanges are preserved. Only the right first wing phalanx is complete, measuring 39.66 mm. The right second wing phalanx is incomplete and disarticulated from the first. The left first wing phalanx is represented by proximal and distal fragments, allowing an estimated length of 42.66 mm. An impression of the proximal part of the left second wing phalanx is preserved, forming an angle of 130° with the first phalanx.

Pelvic girdle The left and right sides are unfused. The anterior process of the ilium is only partially preserved posteriorly; the anterior portion is represented by impressions; it extends over a length equivalent to approximately four dorsal vertebrae. The ischial posterior process is rounded and projects posteriorly. Both prepubes are displaced to the right due to compression, with the left prepubis overlying the right. Each prepubis consists of a fan-shaped anterior portion and a shaft portion. The fan-shaped portion is slightly narrower than the width of the ischium (Fig. 5).

Hindlimb Both hindlimbs in IVPP V23669 are fractured. On the left side, the proximal portion of the femur is preserved, revealing an anteriorly directed femoral head. The mid-shaft of the left femur is visible as an impression, while the distal end is entirely missing. The left tibia and fibula are preserved only distally, and cannot be described. The distal portions of left metatarsals I–IV are also fractured, hindering length comparison, although the distal phalanges and unguals are relatively complete. Metatarsal V is uniform in width. The first phalanx of pedal digit V lies beneath metatarsals I–IV. Its second phalanx is incomplete distally but appears as an elongated, straight bone. The right hindlimb is fractured at the proximal femur and rotated, such that the pes is overlying the right abdominal region. The fractured distal femur, along with the associated tibia, fibula, metatarsals, and phalanges, remains in articulation. The femoral head is obscured by the left prepubis, and its total length is unmeasurable due to the rotation and displacement. The tibia and fibula, though largely complete, are fractured and displaced, with the tibia compressed against the fibula; only their overall length can be estimated. The tarsals remain articulated with the tibia. The distal ends of metatarsals I–IV are missing. Metatarsal V is nearly identical to its left counterpart. The first phalanx of the right pedal digit V is well-preserved. The second phalanx is slightly curved and overlies metatarsals I–IV, preserved mostly as an impression indicating a minimum length of 6.98 mm.

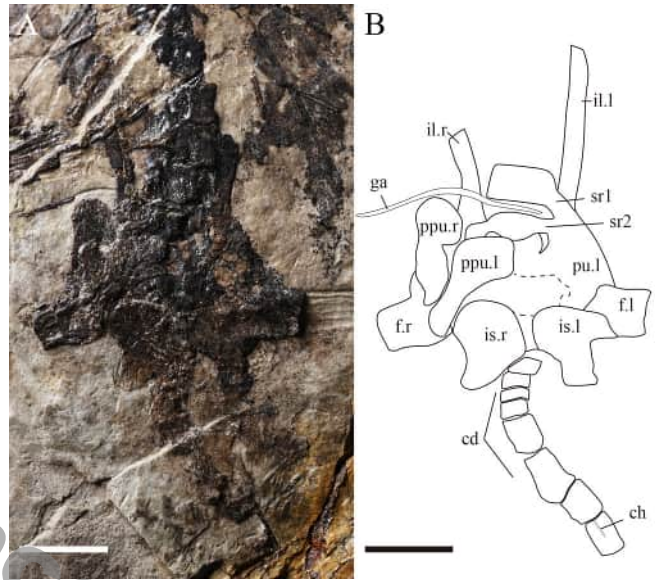

Fig. 5 Photograph (A) and line drawing (B) of the close-up of pelvic girdles of IVPP V23669 from the Middle-Upper Jurassic Qinglong, Hebei

Abbreviations: cd. caudal vertebrae; ch. chevron; f. femur; ga. gastralia; il. ilium; is. ischium; l. left; ppu. prepubis; pu. pubis; r. right; sr. sacral rib. Scale bars equal 5 mm

4.2 IVPP V26040

Ontogenetic status The scapula and coracoid are unfused as in IVPP V23669, and rough articular surfaces are observed on the sternum and limb bones, indicating the specimen is also a juvenile and the bones are incompletely ossified (Fig. 6).

Skull The specimen only preserves a small part of the skull, which is highly compressed. Only a few bones can be identified. The width of the postcranium is 25.79 mm, and it appears that the whole skull must have been wider than the preserved left portion.

Vertebral column The cervical vertebrae are highly compressed. Two bones are tentatively interpreted as cervicals 3 and 4. Cervical vertebrae 3 through 7 are short and robust and all bear large parapophyses. Starting at cervical 4, a longitudinal ridge is present on the central portion of the centrum. The length and width of cervical vertebrae 4 through 6 can be estimated at 2.94 mm and 4.60 mm, respectively. Cervicals 7 and 8 are covered by the coracoid. A rib is present that is approximately half the length of the subsequent ribs, is tentatively identified as that of Cervical 8. The next rib tapers to a point rather than being expanded for articulation similar to the rib of Cervical 9 in the second specimen of *Anurognathus ammoni*, and appears to be double-headed.

The dorsal vertebrae are crushed or covered, but 6 can still be identified. The total length is at least 36.08 mm. All dorsal vertebrae are thinner, with a width of 2.51 mm. Most of the dorsal ribs are preserved as impressions. The prezygapophyses of the first dorsal vertebra are

exposed, although most of the centrum is covered by the sternum, and its length is equal to the length of the preceding vertebrae. At least 9 pairs of ribs anterior to the sacral region can be observed. The first 6 dorsal ribs are straight or slightly curved in the anterior portion of the body, while the remaining 3 posterior ribs are distinctly curved posteriorly. The first to third dorsal ribs are double-headed, with a large concavity between the capitulum and tuberculum. Three rows of gastralia are preserved as impressions.

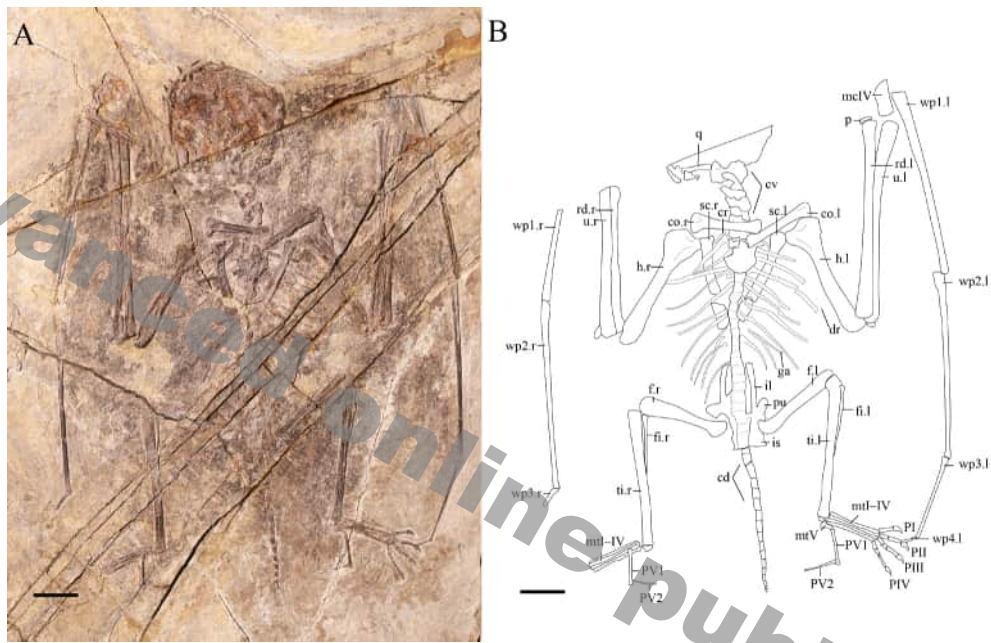

Fig. 6 Photograph (A) and line drawing (B) of the specimen IVPP V26040 from the Middle-Upper Jurassic Linglongta, Liaoning

Abbreviations: cd. caudal vertebrae; co. coracoid; cr. cervical rib; cv. cervical vertebrae; dr. dorsal rib; f. femur; fi. fibula; ga. gastralia; h. humerus; il. ilium; is. ischium; l. left; mcIV. metacarpal IV; mtI–V. metatarsal I–V; p. pteroid; pu. pubis; PI–IV. pedal digits I–IV; PV1 and 2. phalanges 1 and 2 of pedal digit V; q. quadrate; r. right; rd. radius; sc. scapula; ti. tibia; u. ulna; wp1–4. wing phalanges 1–4

Scale bars equal 10 mm

The sacral vertebrae are obscured by compression. It consists of about five vertebrae. They measure 1.86 mm in length, such that the total trunk length from the first dorsal vertebra to the last sacral vertebra measures 13.33 mm.

Caudal vertebrae are well-preserved. There is evidence of at least 17 vertebrae. It is shorter than dorsal series with a length of 33.72 mm. The caudal vertebrae become more elongated posteriorly reaching the maximum length at the 8th caudal vertebra and then becoming shorter towards the distal tip. The last two vertebrae are preserved as impressions in the matrix. Many zygapophyses are visible from the 4th caudal vertebra to the 13th vertebra (Fig. 7A, B).

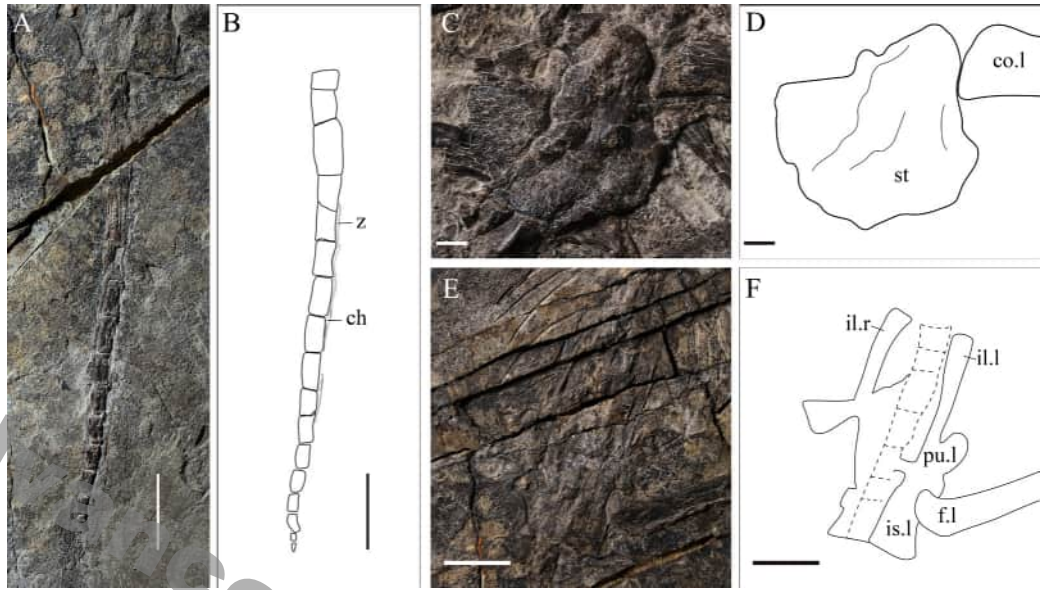

Fig. 7 Close-up photographs (A, C, E) and line drawings (B, D, F) of IVPP V26040 from the Middle-Upper Jurassic Linglongta, Liaoning

A, B. completely preserved tail with zygapophyses and chevrons; C, D. sternum exposed in ventral view; E, F. pelvic girdle. Abbreviations: ch. chevron; co. coracoid; f. femur; il. ilium; is. ischium; l. left; pu. pubis; r. right; st. sternum; z. zygapophyses. Scale bars equal 5 mm (A, B, E and F) and 1 mm (C, D)

Sternum The right part of the sternum is significantly larger than the left, indicating that ossification is incomplete. The cristospine is short and robust, forming a semicircle. Some serrations on the lateral edges appear to represent articulation points for the sternal ribs. The width of the cristospine is 2.20 mm, which is about one-third of the sternal plate width of 6.82 mm. The sternal plate is semicircular in outline, and a thick ridge is visible on the midline. The plate is as long as 3 or 4 of the dorsal vertebrae. There are rough surfaces present on the posterior part of the sternum plate (Fig. 7C, D).

The pterosaurian sternum is typically poorly preserved due to its thin morphology or weak ossification (Hone, 2023). Only two anurognathid sterna have been reported. The sternum is preserved in the second specimen of *Anurognathus ammoni*, although largely obscured by the dorsal vertebrae in dorsal view, and in the holotype of *Bratachognathus volans* (PIN 52-2). In the original publication, Riabinin (1948) reported on the presence of a sternum covered by phalanges. In a reexamination, Bakhurina (1988) determined that this element is part of the right humerus, and that a second bone in the center represents the true sternum; this bone is broadly trapezoid with a deep keel (Bakhurina and Unwin, 1995). Hone (2023) later interpreted the sternum as pentagonal, with the sternal plate slightly wider than long. Comparing the sternum of PIN 52-2 with that of IVPP V26040, both have a short, robust and semicircle cristospine, a thick ridge on the sternal plate (possibly representing impressions from vertebrae), and extensive rough areas on the sternal plate for muscle attachment or cartilaginous extension.

Pectoral girdles The scapula and coracoid are unfused and form a V-shaped girdle. The shaft of the coracoid is essentially straight, with a large tubercle at the glenoid fossa formed by the considerably expanded glenoid end. The left coracoid appears to be in articulation with the sternum. The scapulae have slightly curved shafts. The shaft of the scapula has a relatively deep longitudinal groove. The scapula is slightly longer than the coracoid.

Forelimbs The humerus is straight. Both the proximal and distal articular ends are expanded. The deltopectoral crest is preserved as an impression and appears to be trapezoidal. The ulnar crest is prominent and forms a subtriangular shape. There is a fossa at the proximal end of the humerus. The shafts of the radius and ulna are subequal, straight, and slender and about 1.61 times as long as the humerus. There is a sesamoid at the proximal end of each ulna. The ulna and radius separate at the distal end. The carpals could not be identified. The pteroid is slender and slightly curved. The wing metacarpal is more robust than the other metacarpals. The proximal end of the first wing phalanx is not preserved. Therefore, the length of the 1st wing phalanx is at least 45.16 mm, longer than the 2nd wing phalanx which is 41.84 mm long. The 3rd wing phalanx exhibits a significant reduction, about half the length of the 2nd one. The 4th wing phalanx is only 3.28 mm. The first and second wing phalanges are both gently bowed, while the third is perfectly straight, and the fourth is curved. The joint between the left second and third wing phalanx is preserved at an angle of 160°, whereas the following one is at 130°. On the right side, the third wing phalanx bends outward and forms a 210° angle with the second wing phalanx. However, the elements remain articulated, and it is unclear whether this results from compression or represents the natural in *vivo* posture.

Pelvic girdles The right ischium and pubis have been lost. The preacetabular process of the ilium is slender and long, covering at least 5 posterior dorsal vertebrae. The width is 1.16 mm at the base of the ilium, and thickens anteriorly to a maximum width of 1.79 mm, about 1.5 times the width of the base. The pubis and ischium appear to be unfused (Fig. 7E, F).

Hindlimbs The left femur is preserved in articulation with the pelvis. It is slender and straight, with a modest, dorsally directed femoral head. The fibula is less than half the length of the tibia, strongly expanded at the proximal end and tapering distally. A large proximal tarsal articulated with the distal end of the tibia is visible on both sides. The metatarsals are closely appressed. The length of metatarsal IV is shorter than that of metatarsals II and III. The metatarsal V has a considerably expanded proximal end, that is much wider than the distal end. The pedal digital formula is 2-3-4-5-2. Phalanx 2 of pedal digit V is slender, curved and subequal in size to phalanx 1.

5 Discussion

5.1 Revised skull reconstruction

In previous studies, the skull morphology of *Dendrorhynchoides* and was not clearly

differentiated. For *Luopterus* and *Vesperopterylus*, detailed cranial descriptions are limited by poor preservation. Here we revised the line drawings of the skulls for these three specimens (*Dendrorhynchoides*, *Luopterus* and *Jeholopterus*) (Fig. 8). These revisions integrate osteological identifications from the description (see above).

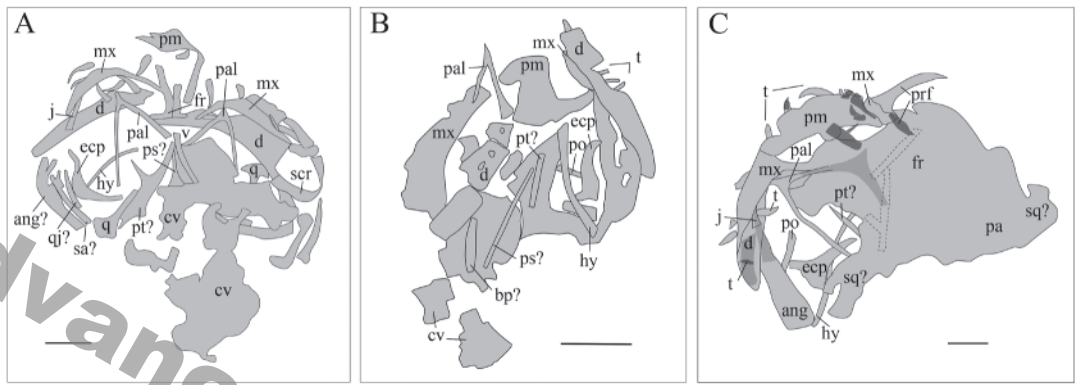

Fig. 8 The line drawings of the skulls of other anurognathids

A. *Dendrorhynchoides* (GMV 2128); B. *Luopterus* (JZMP-04-07-3); C. *Jeholopterus* (IVPP V12705) (the light grey denotes areas preserved as impressions on V12705B, dark grey denotes areas represented by preserved bone, and dashed lines indicate regions where the bone shape is discernible beneath overlying elements)
Abbreviations: ang. angular; bp. basipterygoid; cv. cervical vertebrae; d. dentary; ecp. ectopterygoid; fr. frontal; hy. hyoid; j. jugal; mx. maxilla; pa. parietal; pal. palatine; pm. premaxilla; po. postorbital; prf. prefrontal; ps. parasphenoid; pt. pterygoid; q. quadrate; qj. quadratojugal; sa. surangular; scr. sclerotic ring; sq. squamosal; t. tooth; v. vomer. Scale bars equal 2 mm (B) and 5 mm (A, C)

In both *Dendrorhynchoides* and *Jeholopterus*, the mandible is markedly fractured, similar to that in IVPP V23669. However, no dental elements are preserved on the posterior mandibular fragments. Accordingly, the dentary and angular have been delineated and labeled separately in the revised reconstructions.

Integrating the reinterpretations from this description, a revised reconstruction of the anurognathid skull is proposed herein based on the reconstructions of Bennett (2007) and Dalla Vecchia (2022) (Fig. 9). In the revised reconstruction, the prefrontal is added, the identification of the squamosal is corrected, the jugal is repositioned, and the inferred quadratojugal is included. Dentition follows IVPP V23669 (no mandibular teeth for clarity). In the revised palatal reconstruction, the vomer/pterygoid morphology is revised and the ectopterygoid is added. Posterior palatal contacts remain uncertain due to poor preservation. The parasphenoid is tentatively included in the occipital region, based on comparison with *Dendrorhynchoides* and *Luopterus*.

5.2 Teeth

Tooth counts vary among anurognathid genera. For *Anurognathus*, Wellnhofer (1975) originally described the holotype as having three premaxillary and five maxillary teeth; this count was later revised by Bennett (2007) to three premaxillary and six maxillary teeth.

Batrachognathus possesses three premaxillary teeth (Riabinin, 1948). Dalla Vecchia (2022) illustrated eight paired maxillary teeth, consistent with the total of eleven teeth reported by Unwin and Bakhurina (2000), with clear interdental spacing. In *Sinomacrops*, the maxilla bears nine alveoli, though the premaxillary count remains uncertain. *Dendrorhynchoides* preserves two premaxillary teeth, two left maxillary teeth, one right maxillary tooth, and three left mandibular teeth. *Cascocauda* was described with nineteen identifiable teeth; re-examination suggests the right premaxilla is separated from the maxilla and bears three sets of teeth per side, with the right maxilla exhibiting potentially paired, similarly oriented teeth similar to those in IVPP V23669. Only four teeth of indeterminate position can be seen in *Luopterus*. *Jeholopterus* preserves two teeth on the left premaxilla and three on the right (the middle one may be from dentary). However, only the first right premaxillary tooth is complete. The anteriormost preserved tooth on the left is situated posterior to the first right premaxillary tooth and may represent the second left premaxillary tooth. A portion of a tooth corresponding to this element is preserved on the top slab (IVPP V12705B). *Vesperopterylus* was initially described in ventral view with eight teeth—slender, rod-like premaxillary teeth and stouter, blunter-tipped maxillary teeth. Re-examination suggests the exposed elements are more likely mandibles in dorsal view, with some possible premaxillary remnants; preservation is too poor for definitive counts.

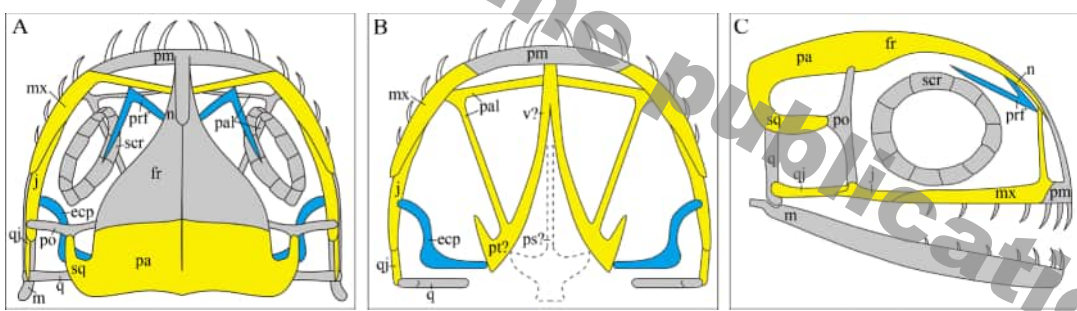

Fig. 9 Reconstruction of anurognathids, redrawn and modified from Bennett (2007) and Dalla Vecchia (2022)
Blue areas indicate newly added elements; yellow areas indicate revised regions
A. dorsal view; B. ventral view; C. right lateral view. Abbreviations: ecp. ectopterygoid; fr. frontal; j. jugal; m. mandible; mx. maxilla; n. nasal; pa. parietal; pal. palatine; pm. premaxilla; po. postorbital; prf. prefrontal; ps. parasphenoid; pt. pterygoid; q. quadrate; qj. quadratojugal; scr. sclerotic ring; sq. squamosal; v. vomer
Not drawn to scale

In this study, we compiled data on the dental counts, premaxillary tooth length, and skull length of anurognathids. Skull length was included for comparison because some large-bodied adult individuals exhibit relatively small skull sizes (Table 1).

The analysis reveals that, apart from *Batrachognathus volans* (PIN 52-2)—which has a higher tooth count relative to its larger skull—only *Sinomacrops bondei* exhibits a dentition substantially more numerous than other anurognathids. Comparison of published figures with other specimens suggests potential issues with the originally reported number of alveoli.

First, the undulating surface along the maxilla (identified as the jugal in the *Sinomacrops* description) is also present in *Dendrorhynchoides* and *Jeholopterus*, raising the possibility that surface depressions were misinterpreted as alveoli. Furthermore, interdental spacing in other anurognathids is markedly wider than in *Sinomacrops* (when the closely paired teeth in *Cascocauda* and IVPP V23669 are considered as single replacement sets). Therefore, the alveolar count in *Sinomacrops* may require reevaluation and confirmation from additional specimens. If the questionable alveoli in *Sinomacrops* are excluded, a positive correlation between tooth number and skull length appears plausible among anurognathids. However, this trend remains tentative due to insufficient supporting evidence.

Table 1 Tooth counts and the measurements of teeth and skulls for anurognathids (mm)

Taxon	Specimen	pmt	mxt	dt	pmt length	skull length
Anurognathus ammoni	BSP 1922 I 42	3	6	>3	2.7	~27
	SMNS 81928	–	–	–	–	15.3
Batrachognathus volans	PIN 52-2	3	8	–	3.2	48
Dendrorhynchoides curvidentatus	GMV 2128	>2	>2	>3	3.03	>17.85
Jeholopterus ningchengensis	IVPP V12705	3	>3	>1	3.85	28
	CAGS-Z070	3	>3	–	–	21.1
Luopterus mutoudengensis	JZMP-04-07-3	–	–	>4	–	24.75
Vesperopterylus lamadongensis	BMNHC-PH-001311	–	–	–	3.51	31.8
Sinomacrops bondei	JPM-2012-001	–	9	–	–	>16.26
Cascocauda rong	NJU-57003	3	>3	–	>2.87	22.2
	IVPP V23669	3	4	7	3.27	>19
indeterminate	IVPP V16728	–	–		3.1	–

Abbreviations: dt. dentary tooth; mxt. maxillary tooth; pmt. premaxillary tooth.

Premaxillary tooth length shows little variation among anurognathid genera and body sizes. The teeth of *Vesperopterylus* were previously described as relatively stout with blunter tips, unlike the slender, recurved teeth of *Dendrorhynchoides*. However, this difference may be largely perceptual: the much smaller skull of *Dendrorhynchoides* could make its teeth appear slenderer. Re-examination shows that *Vesperopterylus* teeth also have curved tips. Similarly, *Anurognathus*, whose teeth were described as pupiform, also exhibits slender, curved teeth in the left posterior region of the skull in specimen SMNS 81928—demonstrating that slender, recurved teeth are not uncommon in this group.

Based on the preceding discussion, it is hypothesized that anurognathids possessed three slender, anteriorly curved premaxillary teeth per side. The maxilla bore a variable number of teeth (4–9), all shorter than the premaxillary teeth. The mandibular condition observed in IVPP V23669—where anterior teeth are slightly shorter than the premaxillary teeth, decreasing in length posteriorly, and culminating in short, robust, hook-shaped posterior teeth—may also be common to the clade. Tooth size appears to have changed little during ontogeny. The closely paired teeth, potentially representing replacement sets, observed in *Cascocauda* and IVPP V23669 have not been confirmed in other specimens and require verification from more complete material.

5.3 Cervical rib

Cervical ribs are typically poorly preserved in anurognathids. They were previously reported only in *Anurognathus* and *Jeholopterus*, in which Bennett (2007) described two cervical ribs in *Anurognathus*: the eighth cervical rib is slenderer than the subsequent ribs and is about one-half the length of the ninth cervical rib, which is nearly the same length as the first dorsal rib. Both taper distally without expansion for articulation. *Jeholopterus* was described as having short, slender cervical ribs.

Re-examination of anurognathid material confirms that cervical ribs are indeed rarely observable. However, the eighth cervical rib (approximately half the length of the subsequent rib) described by Bennett can now be confirmed in *Jeholopterus*, *Luopterus*, and *Cascocauda*. In *Jeholopterus* (IVPP V12705B), the eighth cervical rib is present, and the following rib also tapers distally without articular expansion, supporting its identification as the ninth cervical rib; their length is about 14.65 mm and 23.27 mm, resulting in the ninth cervical rib being 1.58 times the length of the eighth. A well-preserved double-headed rib is present on the right ninth cervical rib in this specimen. In *Luopterus*, the eighth cervical rib is preserved as an impression, and the following rib also shows distal tapering. *Cascocauda* reveals a previously unillustrated, relatively short rib on the left side. It is distinctly shorter than the subsequent rib and is therefore identified as the eighth cervical rib. The following rib, as in other specimens, shows no distal expansion and is identified as the ninth cervical rib. In *Vesperopterylus*, two of the ribs previously cataloged within the dorsal series exhibit distal tapering, a morphology indicative of cervical ribs. The shorter and more anterior of these two elements is interpreted as the eighth cervical rib. Similarly, both the eighth and ninth cervical ribs are identifiable in IVPP V26040 and V23669.

The condition described by Bennett (2007)—"The ventral ends of these elongate cervical ribs taper to a point rather than being expanded for articulation. The rib of Cervical 8 is slenderer than the subsequent ribs and is about one-half the length of the rib of the ninth cervical, which in turn is nearly the same length as the first dorsal rib"—appears to be widespread across Anurognathidae. The presence of an eighth cervical rib that is shorter than the subsequent rib is likely a general feature of the clade.

Dalla Vecchia (2022) noted that the short, robust cervical vertebrae and reduced cervical ribs in anurognathids resemble the condition in *Scaphognathus crassirostris* and *Rhamphorhynchus muensteri*. In fact, anurognathid cervical morphology aligns more closely with *Scaphognathus crassirostris*, particularly the juvenile specimen described by Bennett (2014). This juvenile specimen lacks cervical ribs on Cervical 3–8, possessing only a slender rib on Cervical 9 —a pattern similar to the presence of only the eighth and ninth cervical ribs in anurognathids. However, in adult *Scaphognathus crassirostris*, small, double-headed cervical ribs are present on Cervical 4–8 (with the third cervical uncertain) (Wellnhofer, 1975; Bennett,

2014). In contrast, the well-preserved cervical series of the adult anurognathid *Vesperopterylus* clearly shows that even in adulthood, the mid-cervical vertebrae also lack cervical ribs.

5.4 Deltopectoral crest and ulnar crest

In previous studies, Hone (2020) distinguished anurognathids through the shape of deltopectoral crest, as follows: rounded (or semicircular shaped) in *Anurognathus*, parallelogram in *Batrachognathus*, subtriangular in *Dendrorhynchoides* and *Luopterus*, alate in *Jeholopterus*. However, Wei et al. (2021) redefined the structure as trapezoidal in *Anurognathus* and *Jeholopterus*. They added deltopectoral crest morphologies for other reported anurognathids: trapezoidal in *Vesperopterylus*, subrectangular in *Sinomacrops*, and subtriangular in NJU-57003 (the holotype of *Cascocauda rong*). Wei et al. (2021) additionally documented variation in ulnar crest shape: elongated and oblique to the humeral shaft in *Anurognathus* and *Vesperopterylus*, rounded in *Batrachognathus* and *Sinomacrops*, subtriangular in *Dendrorhynchoides*, and reduced but prominent in *Jeholopterus*.

Here we revise the comparative humeral morphology of anurognathids (Fig. 10). Because So et al. (2023) illustrated only one side of the specimen, we refer to the photos by Gao et al. (2009). In the line drawing of the *Dendrorhynchoides* humerus by Wei et al. (2021), the depicted morphology shows discrepancies from the actual left humerus in the specimen, which we revise here (Fig. 10). The humerus of the holotype of *Jeholopterus* (IVPP V12705A) is partially preserved in the counter slab (IVPP V12705B) (Kellner et al., 2010); the two parts were integrated for the revised reconstruction.

In SMNS 81928 (*Anurognathus*) (Fig. 10A, B), the left humerus exhibits a faint, sloping ulnar crest, whereas the right ulnar crest is rounded and less prominent than in the holotype; its orientation relative to the shaft is ambiguous. Similarly, the ulnar crest is rounded in the right humerus of *Luopterus* (Fig. 10F). In *Dendrorhynchoides* (Fig. 10J), the ulnar crest is not triangular as described by Wei et al. (2021) but rather forms a sloping projection. In IVPP V23669 (Fig. 10D, E), the left and right ulnar crests show different morphologies. Based on the preserved portion, the left ulnar crest of IVPP V23669 is gently rounded, while the right is elongated and oriented oblique to the humeral shaft. This variability indicates that the morphology of the ulnar crest is highly susceptible to distortion, often due to compression from the overlying scapula, which is preserved in close proximity in many specimens. The rounded ulnar crest in *Batrachognathus* and *Sinomacrops* is likely also a preservational artifact. In *Batrachognathus*, the humerus lies near the slab margin, and its ulnar crest may not be completely preserved. In *Sinomacrops*, the left humerus is clearly compressed against the scapula, while the ulnar crest on the right humerus shows a distinct sloping margin. Therefore, the rounded morphology of the ulnar crest cannot be confidently regarded as a definitive characteristic in *Batrachognathus* and *Sinomacrops*.

However, in more mature individuals, the ulnar crest appears more prominent and

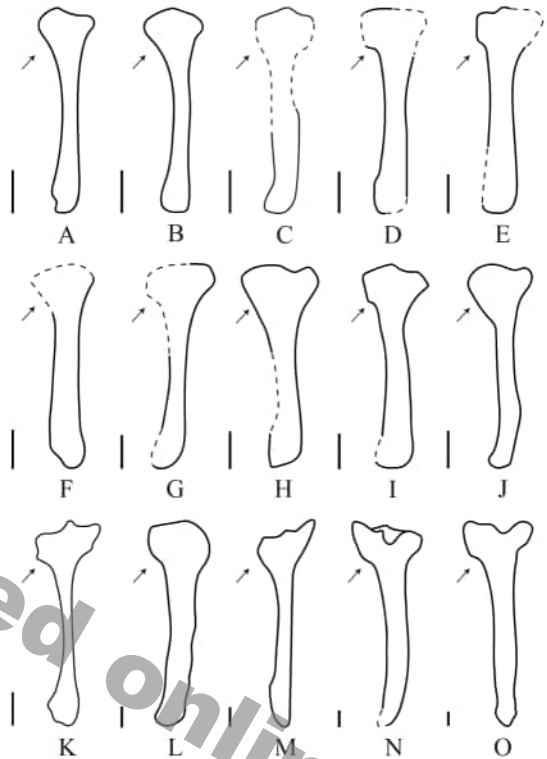

Fig. 10 The line drawings of anurognathid humeri, the arrows indicate the deltopectoral crests and the opposing structure the ulnar crests

A. left humerus of *Anurognathus ammoni* (SMNS 81928); B. right humerus of *A. ammoni* (SMNS 81928); C. left humerus of *Sinomacrops bondei* (JPM-2012-001); D. left humerus of IVPP V23669; E. right humerus of IVPP V23669; F. right humerus of *Luopterus mutoudengensis* (JZMP-04-07-3); G. left humerus of *Cascocauda rong* (NJU-57003); H. right humerus of *C. rong* (NJU-57003); I. left humerus of IVPP V26040; J. left humerus of *Dendrorhynchoides curvidentatus* (GMV 2128); K. left humerus of *A. ammoni* (BSP 1922 I 42); L, left humerus of *Batrachognathus volans* (PIN 52-2); M. left humerus of *Jeholopterus ningchengensis* (CKGP 19960828) (based on Gao et al., 2009); N. left humerus of *J. ningchengensis* (IVPP V12705); O. right humerus of the holotype specimen of *Vesperopterylus lamadongensis* (BMNHC-PH-001311)

Scale bars equal 5 mm

sloping compared to juveniles. Most reported anurognathid specimens represent juvenile or subadult individuals; only *Jeholopterus* and *Vesperopterylus* can be confidently identified as adults. Although the ontogenetic stage of CKGP 19960828 was not assessed in its original description, its fused scapulocoracoid and relatively larger size suggest it is likely a near-adult individual. In specimen IVPP 12705A (*Jeholopterus*) (Fig. 10N), both ulnar crests are obscured by the coracoid, but the visible portions and that of the Korean specimen CKGP 19960828 (Fig. 10M) imply that the ulnar crest in *Jeholopterus* is also prominent and sloping, similar to *Anurognathus* and *Vesperopterylus* (Fig. 10K, O). While the maturity of BSP 1922 I 42 (*Anurognathus*) remains uncertain, it is markedly more mature than SMNS 81928 (being nearly twice the size). When the ulnar crests of anurognathids are compared across ontogenetic

stages, a clear trend emerges: larger, more mature individuals exhibit a more distinct, sloping ulnar crest, whereas in smaller, younger individuals, the presence of morphological differences is difficult to assess.

The deltopectoral crest in NJU-57003 (*Cascocauda*) (Fig. 10G, H) exhibits two different morphologies: the left exhibits a marked projection from the shaft and tends to be rounded, while the right is smooth, forming a triangle at the proximal end. These observations show that the deltopectoral crest was significantly compressed during the preservation process. A similar range of variations is observed in other anurognathid specimens. Some exhibit a distinct, projecting crest that forms a trapezoidal or parallelogram-shaped profile (Fig. 10D, E, I, K, N, O), while others show a smoother transition resulting in a more triangular or rounded margin (Fig. 10A, B, C, F, J, L, M). This is unlikely due to taxonomic differences and is more plausibly attributed to varying degrees of post-mortem deformation. Notably, the deltopectoral crest of BSP 1922 I 42 (*Anurognathus*) (Fig. 10K) is more trapezoidal than that of the smaller specimen SMNS 81928 (*Anurognathus*) (Fig. 10A, B). When evaluated within an ontogenetic framework, a pattern emerges similar to that for the ulnar crest: larger, more mature individuals tend to possess a more projecting, trapezoidal deltopectoral crest.

In summary, the deltopectoral and ulnar crest of smaller, juvenile anurognathids are highly susceptible to compression from adjacent bones and sediment. In contrast, these features are more consistently preserved in larger, more mature individuals with a higher degree of ossification. Furthermore, the observed morphological variation suggests a possible ontogenetic trend: the deltopectoral crest may tend to become trapezoidal during growth, while the adult ulnar crest trends toward a more sloping, prominent orientation relative to the humeral shaft.

5.5 Tail

Even though specimens of anurognathids are rare, tail morphology reportedly varies. Döderlein (1923) and Wellnhofer (1975) described the holotype of *Anurognathus ammoni* as possessing 11 caudal vertebrae. However, Bennett (2007) reinterpreted the specimen as having only 7 caudal vertebrae preserved but suggested that the tail is incomplete. The second specimen has 9 caudal vertebrae ending in a flat articular surface. *Dendrorhynchoides* was mistakenly described as having a long tail (Ji and Ji, 1998). Unwin and Bakhurina (2000) suggested that it had a short tail consisting of at least 6 and possibly up to 8 caudal vertebrae, noting that the elongate distal section of the tail had been artificially added to the fossil. The re-examination of Hone (2020) suggests that there are structures distal to this tail that include genuine bone. For a decade following, the absence of tails in the holotypes of *Batrachognathus* and *Jeholopterus* led to the widespread assumption that all anurognathids possessed a short tail as in *Anurognathus*. This view was challenged when Lü and Hone (2012) described *Luopterus*, which preserves an incomplete tail of at least 15 vertebrae, measuring about 85% of the femur

length. Subsequently, Costa et al. (2013) reported a new specimen of *Batrachognathus* (PIN 2585/4) with a tail length of at least 44 mm, exceeding its humerus length. Further discoveries confirmed long-tailed morphologies in other taxa: IVPP V16728 possesses a 29.3 mm tail (~1.5 times femur length) comprising 20 vertebrae (Jiang et al., 2015); *Cascocauda* has a tail of at least 20 vertebrae that is 42 mm in length (Yang et al., 2021); *Sinomacrops* exhibits a tail impression distinctly longer than the femur, though the vertebral count is indeterminate (Wei et al., 2021). As noted in the preceding sections, IVPP V26040 preserves approximately 17 caudal vertebrae and V23669, while incomplete, clearly indicates an elongate tail.

During this study, the contentious tail morphology of *Dendrorhynchoides*, *Jeholopterus*, and *Luopterus* was re-examined. In *Dendrorhynchoides*, Hone's (2020) interpretation that the distal segment represents the genuine tail is supported. Measurement yields a total tail length of approximately 43.61 mm. No traces of zygapophyses or chevrons were observed, likely due to poor preservation. Lü and Hone (2012) inferred the tail length of the *Jeholopterus* holotype based on slightly visible impressions and the apparent presence of surrounding pycnofibers, suggesting it was comparable to the femur length. Examination reveals that the presence of hindlimbs and extensive soft tissues in the caudal region obscures any definitive tail impressions or associated fibers, rendering this conclusion unsubstantiated. The referred specimen CAGS-Z070 preserves a relatively short tail; in CKGP 19960828 the tail is proximally broken and the distal portion is missing. Consequently, *Jeholopterus* is interpreted here as having a short tail. Reobservation of *Luopterus* reveals impressions consistent with possible chevrons among the caudal vertebrae. Although the tail is incomplete, the size of the preserved distal elements suggests its total length probably did not exceed that of the dorsal vertebral series and may have been similar to, or shorter than, the femur.

6 Conclusion

This study provides a comprehensive description of the osteological morphology of two anurognathid pterosaur specimens from the Yanliao Biota. For the first time, CT scanning and reconstruction were applied to a relatively well-preserved anurognathid skull. This approach has significantly aided in the separation and identification of skull elements. Additionally, the skulls of previously reported anurognathid specimens were reanalyzed and revised reconstructions are presented. More detailed discussions were conducted concerning dentition, cervical ribs, the deltopectoral crest, and caudal morphology. Problematic measurement data were also corrected and updated.

Acknowledgements This manuscript is dedicated to Prof. Chang Meemann, who has generously supported our pterosaur research. We had the honor of naming *Gegepterus changae* after her in 2007. We thank Xiang Long for preparing the specimens, Song Junyi and Xu Yizhi

for their helpful discussions, and Hou Yemao and Yin Pengfei for their assistance with CT scanning (IVPP). We also thank Zhang Yuguang and Liu Di (NHMC), Liu Fengxiang and Tan Kai (GMC), Sun Zhenyuan and Wang Cai (JZMP), Zhang Ying, Li Xuemin, and Lü Huiwen (Changyang Paleontological Museum) and O. W. M. Rauhut (BSP) for kindly providing access to the specimens. This work was supported by the National Natural Science Foundation of China (42072017, 42288201, and 42572026).

燕辽生物群的两件蛙嘴翼龙类新标本及对蛙嘴翼龙类头骨的新解释

佟仕达[1,2] 蒋顺兴[1] 程 心[3] 汪筱林[1,2]

(1 中国科学院古脊椎动物与古人类研究所，脊椎动物演化与人类起源重点实验室 北京 100044)

(2 中国科学院大学地球与行星科学学院 北京 100049)

(3 吉林大学地球科学学院 长春 130061)

摘要：蛙嘴翼龙是一类从中侏罗世到早白垩世时期分布于欧亚大陆的小型非翼手龙类翼龙。其主要的鉴别特征是短而宽的头骨，这一形态与所有其他翼龙类群都不同。由于保存的原因，蛙嘴翼龙类的头骨结构长期以来一直都存在争议。详细描述了两件来自燕辽生物群髫髻山组的蛙嘴翼龙类标本。并对其中一件标本中保存相对完好的头骨进行了计算机断层扫描与重建。结果显示，该头骨存在一个与大部分翼龙都不相同的独特的骨骼结构，其功能可能类似其他爬行类的眶上骨。基于对该标本头骨的研究，对之前未详细描述的其他蛙嘴翼龙类头骨进行了修订，最终重建了一个新的蛙嘴翼龙类头骨复原图。同时还对蛙嘴翼龙类的头后骨骼部分进行了更为全面的比较分析和讨论。

关键词：燕辽生物群，髫髻山组，翼龙，蛙嘴翼龙类，古尾翼龙属

References

Andres B B, 2010. Systematics of the Pterosauria. Ph. D thesis. New Haven: Yale University. 1–366

Bakhurina N N, 1988. On the first rhamphorhynchoid from Asia: *Batrachognathus volans* Ryabinin 1948, from Upper Jurassic beds of Karatau. Byull Moskovsk Obshch Isp Prir Otd Geol, 63(5): 132

Bakhurina N N, Unwin D M, 1995. A survey of pterosaurs from the Jurassic and Cretaceous of the former Soviet Union and Mongolia. Hist Biol, 10: 197–245

Bennett S C, 2007. A second specimen of the pterosaur *Anurognathus ammoni*. Paläont Z, 81(4): 376–398

Bennett S.C, 2014. A new specimen of the pterosaur *Scaphognathus crassirostris*, with comments on constraint of cervical

vertebrae number in pterosaurs. N Jb Geol Paläont Abh, 271(3): 327–348

Costa F R, Alifanov V, Dalla Vecchia F M et al., 2013. On the presence of an elongated tail in an undescribed specimen of *Batrachognathus volans* (Pterosauria: Anurognathidae: Batrachognathinae). In: Sayão J M, Costa F R, Bantim R A M et al. eds. Short Communications, Rio Ptero 2013 – International Symposium on Pterosaurs. Rio de Janeiro: Universidade Federal do Rio de Janeiro, Museu Nacional. 54–56

Dalla Vecchia F M, 2009. Anatomy and systematics of the pterosaur *Carniadactylus* gen. n. *rosenfeldi* (Dalla Vecchia, 1995). Riv Ital Paleontol Stratigr, 115(2): 159–188

Dalla Vecchia F M, 2019. *Seazzadactylus venieri* gen. et sp. nov., a new pterosaur (Diapsida: Pterosauria) from the Upper Triassic (Norian) of northeastern Italy. PeerJ, 7: e7363

Dalla Vecchia F M, 2022. The presence of an orbitalantorbital fenestra: further evidence of the anurognathid peculiarity within the Pterosauria. Riv Ital Paleont Stratigr, 128(1): 23–42

Döderlein L, 1923. *Anurognathus ammoni*, ein neuer Flugsaurier. Sitzungsber Bayer Akad Wiss, 1923: 117–164

Gao K Q, Li Q G, Wei M R et al., 2009. Early Cretaceous birds and pterosaurs from the Sinuiju Series, and geographic extension of the Jehol Biota into the Korean Peninsula. J Paleont Soc Korea, 25(1): 57–61

Hone D W E, 2020. A review of the taxonomy and palaeoecology of the Anurognathidae (Reptilia, Pterosauria). Acta Geol Sin, 94(5): 1676–1692

Hone D W E, 2023. The anatomy and diversity of the pterosaurian sternum. Palaeontol Electron, 26(1): a12

Ji Q, Yuan C X, 2002. Discovery of two kinds of protofeathered pterosaurs in the Mesozoic Daohugou Biota in the Ningcheng region and its stratigraphic and biologic significances. Geol Rev, 48(2): 221–224

Ji S A, Ji Q, 1998. A new fossil pterosaur (Rhamphorhynchoidea) from Liaoning. Jiangsu Geol, 22: 199–206

Ji S A, Ji Q, Padian K, 1999. Biostratigraphy of new pterosaurs from China. Nature, 398: 573

Jiang S X, Wang X L, Cheng X et al., 2015. Short note on an anurognathid pterosaur with a long tail from the Upper Jurassic of China. Hist Biol, 27(6): 717–721

Kellner A W A, 2003. Pterosaur phylogeny and comments on the evolutionary history of the group. Geol Soc Lond Spec Publ, 217(1): 105–137

Kellner A W A, Wang X L, Tischlinger H et al., 2010. The soft tissue of *Jeholopterus* (Pterosauria, Anurognathidae, Batrachognathinae) and the structure of the pterosaur wing membrane. Proc R Soc B, 277: 321–329

Kubota M, Hallermann J, Beerlink A et al., 2024. The skull morphology of the Komodo dragon, *Varanus komodoensis* (Reptilia, Squamata, Varanidae)—A digital-dissection study. Evol Syst, 8: 219–245

Lü J C, Hone D W E, 2012. A new Chinese anurognathid pterosaur and the evolution of pterosaurian tail lengths. Acta Geol Sin, 86(6): 1317–1325

Lü J C, Ji Q, 2006. Preliminary results of a phylogenetic analysis of the pterosaurs from western Liaoning and surrounding areas. J Paleont Soc Korea, 22(1): 239–261

Lü J C, Meng Q J, Wang B P et al., 2017. Short note on a new anurognathid pterosaur with evidence of perching behaviour from Jianchang of Liaoning Province, China. Geol Soc Lond Spec Publ, 455: 95–104

Ősi A, 2010. Feeding-related characters in basal pterosaurs: implications for jaw mechanism, dental function and diet. Lethaia, 44(2): 136–152

Riabinin A N, 1948. Remarks on a flying reptile from the Jurassic of the Kara-Tau. Akad Nauk Paleontol Inst Trudy, 15(1): 86–93

Sangster S, 2021. The osteology of *Dimorphodon macronyx*, a non-pterodactyloid pterosaur from the Lower Jurassic of

Dorset, England. Palaeontogr Soc Monogr, 175: 1–48

So K S, Kim P H, Won C G, 2023. First articulated rhamphorhynchoid pterosaur from the Early Cretaceous of the Democratic People's Republic of Korea. Paleontol J, 57(S1): S90–S94

Unwin D M, 2003. On the phylogeny and evolutionary history of pterosaurs. Geol Soc Lond Spec Publ, 217(1): 139–190

Unwin D M, Bakhurina N N, 2000. Pterosaurs from Russia, Middle Asia and Mongolia. In: Benton M J, Shishkin M A, Unwin D M et al. eds. The Age of Dinosaurs in Russia and Mongolia. Cambridge: Cambridge University Press. 420–433

Vidovic S U, Martill D M, 2018. The taxonomy and phylogeny of *Diopecephalus kochi* (Wagner, 1837) and '*Germanodactylus rhamphastinus*' (Wagner, 1851). Geol Soc Lond Spec Publ, 455: 125–147

Wang X L, Zhou Z H, Zhang F C et al., 2002. A nearly completely articulated rhamphorhynchoid pterosaur with exceptionally well-preserved wing membranes and "hairs" from Inner Mongolia, northeast China. Chinese Sci Bull, 47(3): 226–230

Wang X L, Kellner A W A, Jiang S X et al., 2009. An unusual long-tailed pterosaur with elongated neck from western Liaoning of China. An Acad Bras Ciênc, 81(4): 793–812

Wang X L, Rodrigues T, Jiang S X et al., 2014. An Early Cretaceous pterosaur with an unusual mandibular crest from China and a potential novel feeding strategy. Sci Rep, 4: 6329

Wang X L, Jiang S X, Zhang J Q et al., 2017. New evidence from China for the nature of the pterosaur evolutionary transition. Sci Rep, 7: 42763

Wei X F, Pêgas R V, Shen C Z et al., 2021. *Sinomacrops bondei*, a new anurognathid pterosaur from the Jurassic of China and comments on the group. PeerJ, 9: e11161

Wellnhofer P, 1975. Die Rhamphorhynchoidea (Pterosauria) der Oberjura-Plattenkalke süddeutschlands Teil II. Palaeontogr Abt A, 148: 132–186

Yang Z, Benton M J, Hone D W E et al., 2021. Allometric analysis sheds light on the systematics and ontogeny of anurognathid pterosaurs. J Vert Paleont, 41(5): e2028796